Failure process and load-displacement relationship of rectangular block and interlocking block walls during in-plane lateral loading

Furukawa, Aiko; Prasetyo, Jefry Johanes; Kiyono, Junji

自然災害科学 *J. JSNDS* **38** 特別号 **25-41** (**2019**)

Failure process and load-displacement relationship of rectangular block and interlocking block walls during in-plane lateral loading

Aiko FURUKAWA[1], Johanes Jefry PRASETYO[1] and Junji KIYONO[1]

Failure process and load-displacement relationship of rectangular block and interlocking block walls during in-plane lateral loading

Aiko FURUKAWA[1], Johanes Jefry PRASETYO[1] and Junji KIYONO[1]

Abstract

We investigated the effectiveness of using interlocking blocks to reinforce masonry structures. In-plane lateral loading tests were conducted on block walls constructed with three types of block shapes: rectangular blocks, I-shaped blocks, and wave-shaped blocks. The failure process and load-displacement relationships of these three masonry wall types were compared under three vertical stress levels: 0.2 N/mm^2, 0.4 N/mm^2, and 0.6 N/mm^2. It was found that the interlocking mechanism had a strengthening effect under a small vertical stress, and that the effectiveness of the interlocking blocks decreased as the vertical stress increased.

Key words : in-plane lateral loading test, masonry wall, rectangular block, interlocking block, failure process, force-displacement relationship

1. Introduction

The collapse of masonry buildings has caused a large number of fatalities during earthquake events (Coburn and Spence, 2002). It has been reported that catastrophic earthquakes account for 60% of worldwide casualties associated with natural disasters (Giardini et al., 2003). Additionally, the collapse of buildings is the primary cause of death and accounts for 75% of earthquake fatalities over the last century (OCHA, 2015).

Masonry is the most commonly used building type in developing countries, owing to its low cost and availability as a construction material. Masonry buildings are intrinsically strong against

[1] Department of Urban Management, Graduate School of Engineering, Kyoto University, Kyoto City, Japan

vertical loads, but weak against lateral loads such as earthquakes. To reduce casualties related to the collapse of masonry buildings during earthquakes, the reinforcement of masonry buildings is necessary. Considering that unreinforced masonry buildings are still used as dwellings, owing to the low cost of the building materials and labor, it is necessary to develop a new reinforcement method that is cost-efficient and easy to implement.

Many studies have investigated a method of reinforcing masonry structures. A reinforcement method using vertical steel ties (Darbhanzi et al., 2014), a method using fiber-reinforced plastics (Marcari et al., 2007), a method using scrapped tires as tension materials (Turer and Golalm, 2011), and a retrofitting method using PP bands (polypropylene bands), which are commonly used for packing (Sathiparan et al., 2009), have been proposed. The abovementioned reinforcement methods require reinforcing materials, but are readily available and easy to implement.

In this paper, we introduce a reinforcing method for masonry structures that does not require the use of reinforcement materials. The proposed method utilizes interlocking blocks instead of conventional rectangular blocks. The target structures are newly constructed masonry structures. Special molds are necessary to make interlocking blocks, but once the molds are prepared, interlocking blocks can be made using the same materials as those used for conventional blocks. A masonry wall consisting of rectangular blocks resists lateral loads such as earthquakes by friction force after mortar failure occurs, as shown on the left-hand side of **Fig. 1(a)**. On the other hand, a masonry wall consisting of interlocking blocks resists lateral loads through the resistance exerted by interlocking, in addition to friction force, as shown on the right-hand side of **Fig. 1(a)**. In this manner, we expect interlocking blocks to reinforce the wall by interlocking with the adjacent blocks.

Sanada et al. (2006) conducted experiments on a masonry wall consisting of conventional rectangular blocks and a wall consisting of I-shaped interlocking blocks to compare their performance. The walls were subjected to cyclic lateral loading under a constant axial loading of 20 kN. It was observed that the strength of the interlocking block walls was higher than the strength of conventional block walls. It has also been reported that, in terms of resisting forces, the performance of interlocking blocks depends on the ductility of the block material. Based on experimental results, Sanada et al. (2006) reported that ductile interlocking blocks may be effective in improving a vulnerable unreinforced masonry structure.

Our research group has investigated a reinforcing method using interlocking blocks. First, Furukawa et al. (2018a) conducted diagonal compression tests (**Fig. 1(b)**) on normal masonry walls made of rectangular blocks and on irregular masonry walls made of interlocking blocks, as shown in **Fig. 1(c)**. Two types of rectangular blocks with different heights, and two types of interlocking blocks with different shapes were used. Thus, it was observed that the maximum strength of masonry walls with interlocking blocks is lower than the maximum strength of masonry walls with rectangular blocks. However, the effectiveness of using interlocking blocks is not evident. Finite-element analysis has been conducted to clarify this mechanism. Thus, it has been observed that stress concentration occurs at the interlocking part and causes the failure of the blocks at that part.

Next, Furukawa et al. (2018b) conducted diagonal compression tests on masonry walls made of interlocking blocks with various shapes. I-shaped blocks with a right angle, I-shaped blocks with an obtuse angle, hourglass-shaped blocks with a straight line, and hourglass-shaped blocks with a wavy shape were compared as shown in **Fig. 1(d)**. Thus, it was found that masonry walls made with

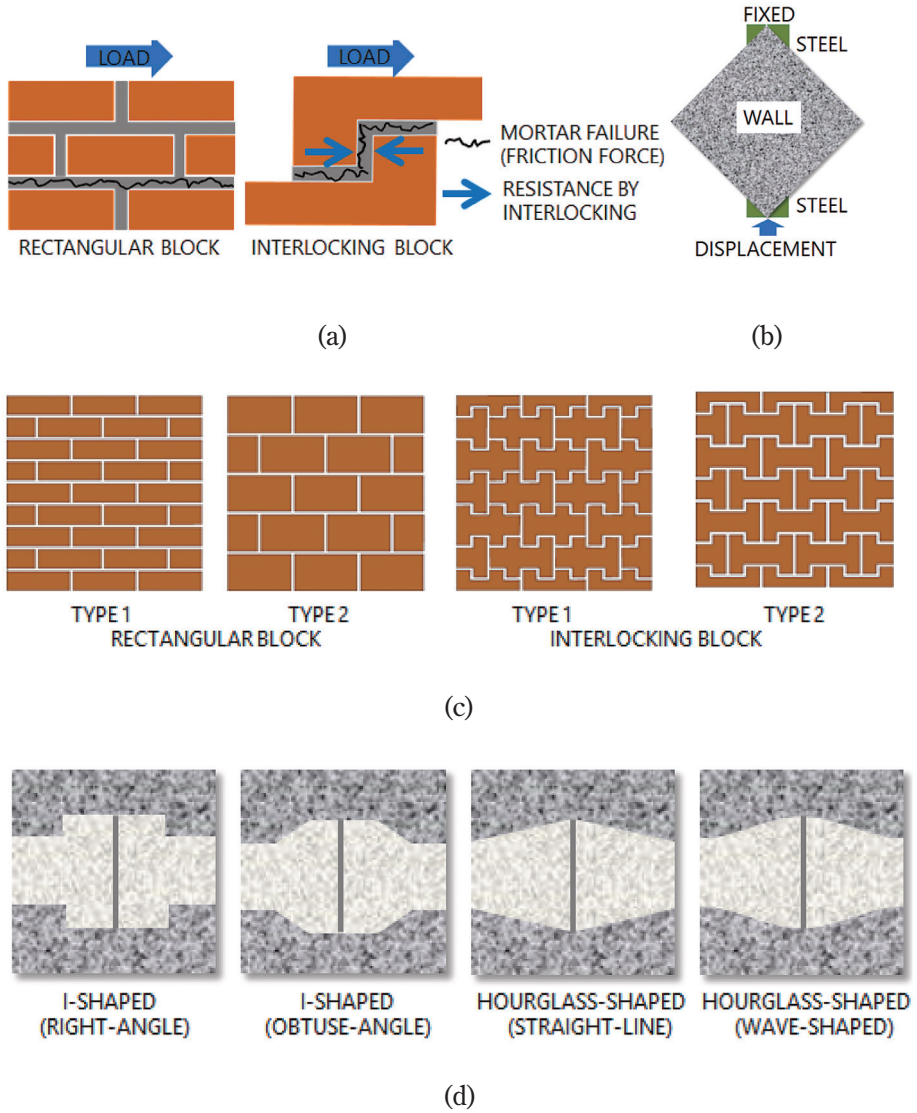

Fig. 1 Diagonal compression tests on interlocking masonry walls carried out in previous studies: (a) difference in the resistance mechanism against lateral load between a masonry wall made with rectangular blocks and a masonry wall made with interlocking blocks; (b) diagonal compression test; (c) rectangular block wall and interlocking block wall test specimens (Furukawa et al., 2018a); (d) test specimens of interlocking brick walls with various block shapes (Furukawa et al., 2018b).

hourglass-shaped blocks have higher strength than walls made with I-shaped blocks. Moreover, a masonry wall made with hourglass-shaped blocks that have a wavy edge has the highest strength amongst all wall types. Furthermore, finite-element analysis has been conducted to clarify the underlying mechanism. The analysis results revealed that walls with I-shaped blocks have lower strength, owing to the stress concentration at the interlocking part. Conversely, walls with hourglass-shaped

blocks have higher strength, owing to lower stress concentration.

The results obtained by the abovementioned experiments have revealed that the performance of an I-shaped interlocking block wall is inferior to the performance of a rectangular block wall. However, the strength of the interlocking block wall increases by using a block shape with lower stress concentration, such as wave-shaped blocks. The experiments conducted previously by our group (Furukawa et al. 2018a; Furukawa et al. 2018b) employed diagonal compression tests (**Fig. 1(b)**), which apply different conditions to the actual seismic loading condition. However, we did not compare the performance between a rectangular block wall and an interlocking block wall with a lower stress concentration. With this background, the objective of this study was to investigate the effectiveness of using interlocking blocks, instead of rectangular blocks, as a reinforcement measure for masonry structures under in-plane lateral loading tests that simulate earthquake loading. Three block shapes, namely, rectangular blocks, I-shaped blocks, and wave-shaped blocks, were compared. To understand the pure effect of the interlocking mechanism, plaster was not used between the blocks. The failure process and load-displacement relationships of the three masonry wall types were compared using the three initial vertical stress levels of 0.2 N/mm^2, 0.4 N/mm^2, and 0.6 N/mm^2, which correspond to the stress affecting the wall of the first floor of two-story, four-story, and six-story masonry buildings, respectively. In this paper, we discuss the effect of the block shape on the performance of a masonry wall under lateral loading.

2. Lateral loading test

2. 1 Test specimen

In this study, a rectangular block, I-shaped interlocking block, and wave-shaped interlocking block were chosen as the subjects of a lateral loading test. **Fig. 2(a)** presents the design document for the masonry walls and the block size. The dimensions of the masonry walls were 24 cm (width) ×30 cm (height) ×10 cm (depth). **Fig. 2(b)** shows the manufactured blocks. Each wall consisted of 12 blocks. There are various possible ways to arrange interlocking blocks, but we considered the simple arrangement shown in **Fig. 2(a)(b)**.

The blocks at the top and bottom had two holes with a diameter of 1 cm, where a steel bar was inserted and connected with the steel frame. In **Fig. 2(a)**, an area with a height of 3 cm at the top and bottom was inside the steel frame. No steel frames were attached to either side of the wall in order to understand the resistance due to pure interlocking between blocks.

In a previous study (Furukawa et al. 2018a), masonry walls were made from burned bricks, and plaster was placed between the adjacent bricks. However, we observed that the variations in block strength and the variations in mortar joint strength also affected the experimental results. Therefore, we thought it necessary to avoid the effect of block strength variations and mortar joint strength variations so as to clarify the pure block shape effect.

To avoid block strength variations, we used mortar blocks. All of the blocks were fabricated simultaneously and under the same conditions. The blocks were made using high-early-strength Portland cement, sand, and water. Specifically, 25% of the material was high-early-strength Portland cement, 60% was sand, and 15% was water. To avoid joint strength variations, plaster was not used.

2. 2 Experimental setup

Fig. 2(c) shows the experimental setup. The wall was installed onto a bottom steel frame, which was fixed under a loading machine. The wall's bottom part with a height of 3 cm was covered by the fixed bottom steel frame, and the wall was fixed to the bottom steel frame using four steel

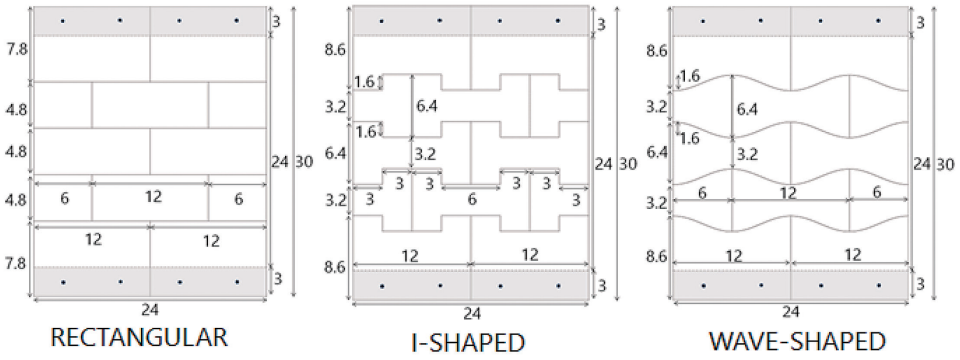

(a)

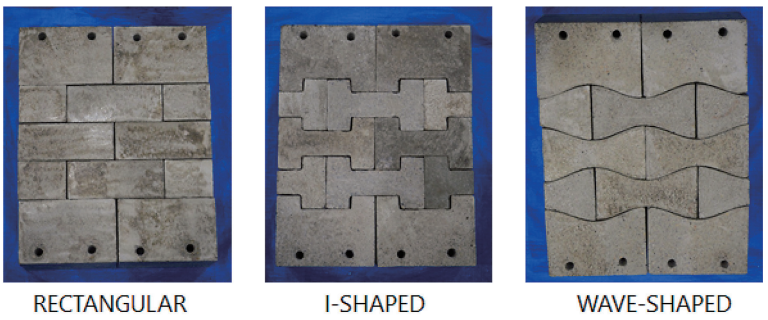

(b)

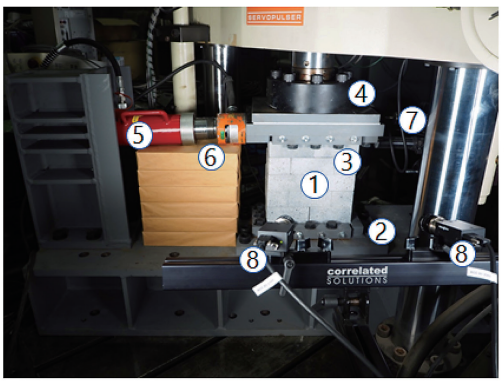

(c)

Fig. 2 Test specimen and experimental setup: (a) design document of the test specimen for each block shape (unit: cm); (b) pictures of each test specimen; (c) experimental setup.

bars and bolts. The wall's top part with a height of 3 cm was also covered by a top steel frame, and the wall was fixed to the top steel frame using four steel bars and bolts. A vertical load was applied to the top steel frame by a vertical loading machine. The vertical displacement and vertical load were measured by the loading machine. A lateral load was applied to the top steel frame using a hydraulic jack. A load cell was installed between the hydraulic jack and the top steel frame to measure the applied lateral load. Displacement transducers were installed at the opposite side of the hydraulic jack to measure the specimen's lateral displacement.

To better understand the specimen's deformation through the entire loading process, the digital correlation system VIC-3DTM (Correlated Solutions) was used. VIC-3D is a powerful system for measuring and visualizing both the strain and movement of the specimen. The VIC-3D system consists of two high-speed cameras, and a software program that analyzes the image data. We captured a picture of the specimen every 0.2 s using the two high-speed cameras. Then, we used the software to compute the strain distribution in the block.

2. 3 Loading conditions

Each wall type was tested under three different vertical loading conditions. This vertical load represents the structural load exerted by the weight above the wall (such as the roof, for example) on the wall itself. The initial vertical stress values and their equivalent conditions are listed in **Table 1**. These values were determined based on the literature (Yamaguchi et al., 2014).

First, we applied a vertical load to the wall specimen by using a displacement-controlled loading machine. We increased the vertical load gradually until the desired initial vertical stress was achieved. Subsequently, the vertical displacement was fixed and maintained constantly throughout the lateral loading test.

Under a constant vertical displacement condition, a gradually increasing lateral load was manually applied to the specimen using the hydraulic jack. In total, nine tests were conducted for the three block shape types, with three levels of initial vertical stresses.

2. 4 Material properties

The material properties are listed in **Table 2**. The density was obtained by averaging the density of all test specimens. Apart from density, the other material properties were determined by averaging the results obtained by the three element tests using cylinder-type test pieces with a diameter of 10 cm and a height of 20 cm. The tensile strength was obtained by conducting a splitting test.

3. Experimental results

3. 1 Rectangular block wall

(1) Results

First, we present the load-displacement relationship in **Fig. 3(a)**. The straight line represents

Table 1 Initial vertical stresses and their equivalent conditions.

Initial Vertical Stress	Equivalent Condition
0.2 N/mm^2	The vertical stress to which the first-floor roof of a two-story building is subjected
0.4 N/mm^2	The vertical stress to which the first-floor roof of a four-story building is subjected
0.6 N/mm^2	The vertical stress to which the first-floor roof of a six-story building is subjected

Table 2 Material properties.

Density (kg/m^3)	Compressive Strength (N/m^2)	Young Modulus (N/m^2)	Poisson's Ratio	Tensile Strength (N/m^2)
2.1×10^3	3.5×10^7	3.0×10^9	0.22	3.3×10^6

the relationship between the lateral load and the lateral displacement, while the dotted line represents the relationship between the vertical load and the lateral displacement. In the cases where the initial vertical stresses were 0.2 N/mm^2 and 0.6 N/mm^2, the lateral and vertical loads gradually decreased, and then maintained a constant value. In the case where the initial vertical stress was 0.4 N/mm^2, both the lateral and vertical loads decreased suddenly after moving by 6 mm, and then became approximately constant. Even though the lateral and vertical loads were not purely constant and decreased gradually or suddenly, in all cases, the wall exhibited sliding movement without cracks forming, regardless of the initial vertical stress. Therefore, the lateral strength was considered to be the force exerted by friction, and the lateral and vertical loads increased as the initial vertical stress increased.

The relationship between the lateral-to-vertical load ratio and the lateral displacement is presented in **Fig. 3(b)**. The lateral-to-vertical load ratio was approximately the same in all cases, and approximately constant throughout the lateral loading. The average lateral-to-vertical load ratio amongst the three cases was calculated as 0.438. Considering that the sliding movement started when the lateral load exceeded the friction limit, the average friction coefficient was determined as 0.438.

The failure process was approximately the same, regardless of the initial vertical stress. An example is presented in **Fig. 4**, which shows the failure process when the initial vertical stress was 0.6 N/mm^2. The top two blocks show the sliding movement above the second-highest blocks. From the lateral-to-vertical load ratio shown in **Fig. 3(b)** and the failure process shown in **Fig. 4**, it can be seen that the sliding movement caused by friction was dominant in the rectangular brick walls.

Fig. 4 also shows the strain contour in the lateral direction. The strain was obtained using the digital correlation system VIC-3DTM (Correlated Solutions). The strain was set to zero when the lateral loading started. Therefore, the figures show the strain increasing or decreasing relative to the initial state. The red color indicates the area where tensile strain was generated. The purple color indicates the area where compressive strain was generated. The green color indicates that the strain was zero or negligible. The top-left block was subjected to compressive strain, owing to the lateral loading (**Fig. 4(a, b, c)**). The top-right block was subjected to tensile strain (**Fig. 4(c)**) because

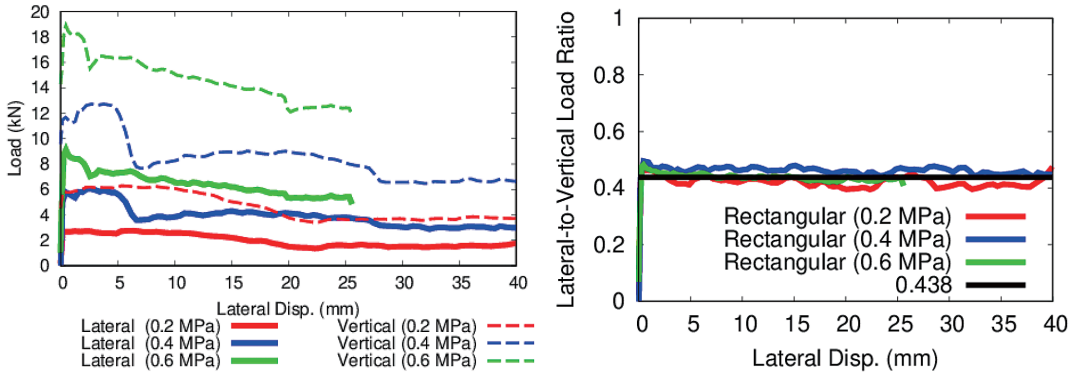

(a) (b)

Fig. 3 Test results for the rectangular block wall: (a) load-displacement relationship; (b) relationship between the lateral-to-vertical load ratio and lateral displacement.

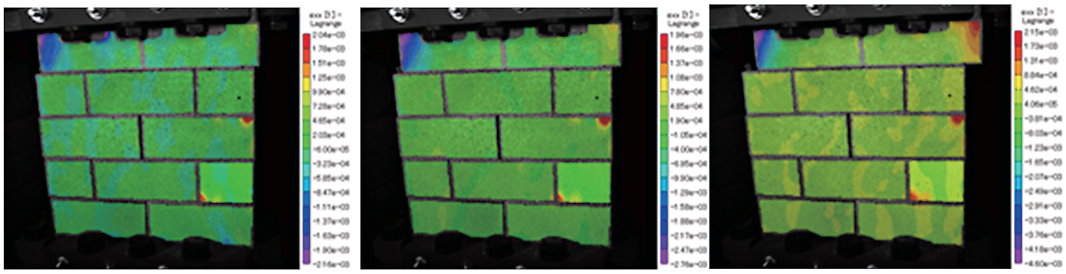

(a) (b) (c)

Fig. 4 Failure process and strain contour in the lateral direction of the rectangular block wall with an initial vertical stress of 0.6 N/mm^2: (a) lateral displacement of 2 mm; (b) lateral displacement of 6 mm; (c) lateral displacement of 12 mm.

the bottom-right part was separated from the block below.

(2) Discussion

The failure process of the rectangular block wall without plaster was the sliding movement caused by the friction failure. The lateral strength was influenced by the friction force. Therefore, the wall with the larger initial vertical stress had the highest lateral strength.

3. 2 I-shaped block wall

(1) Results

The load-displacement relationships of the I-shaped block walls are presented in **Fig. 5(a)**. **Fig. 5(b)** presents the relationship between the lateral-to-vertical load ratio and the lateral displacement. The failure process and strain contour for the three cases are shown in **Figs. 6**, **7**, and **8**. Note that the gray area is the area where the strain shown in **Figs. 6**, **7**, and **8** could not be computed.

First, the results for the initial vertical stress of 0.2 N/mm^2 were investigated. As shown in **Fig. 5(a)**, at an initial vertical stress of 0.2 N/mm^2, the maximum lateral strength of 15.3 kN occurred at a lateral displacement of 21 mm. Before the maximum lateral strength was observed, many other peak loads were observed. At each peak load, a crack formed in the specimen, as shown in **Fig. 6**. This caused the sudden decrease in lateral force. After the maximum strength was reached, the block entered a state of total failure. As shown in **Figs. 5(b)** and **6**, owing to the existence of the interlocking system, the lateral-to-vertical load ratio of the I-shaped brick wall at 0.2 N/mm^2 was higher than that of the rectangular block wall, which was equal to a friction coefficient of 0.438. The higher lateral-to-vertical load ratio represents the strengthening effect of the I-shaped block, in comparison with the rectangular block wall. During the early stages of lateral loading, the interlocking system of the I-shaped block provided the wall with substantial strengthening because the lateral-to-vertical load ratio was much higher than 0.438. However, as cracks began to develop, the strengthening effect exerted by the interlocking system decreased because the lateral-to-vertical ratio gradually decreased and approached a value of 0.438. The sliding movement seen in **Fig. 6** is absent in **Fig. 6(a, b)**, owing to interlocking amongst the elements. A large strain was observed at the interlocking parts, which means that strain concentration occurred at the interlocking parts. Therefore, it is considered that the I-shaped block breaks more easily, owing to the strain concentration at the interlocking parts. The interlocking mechanism increased the

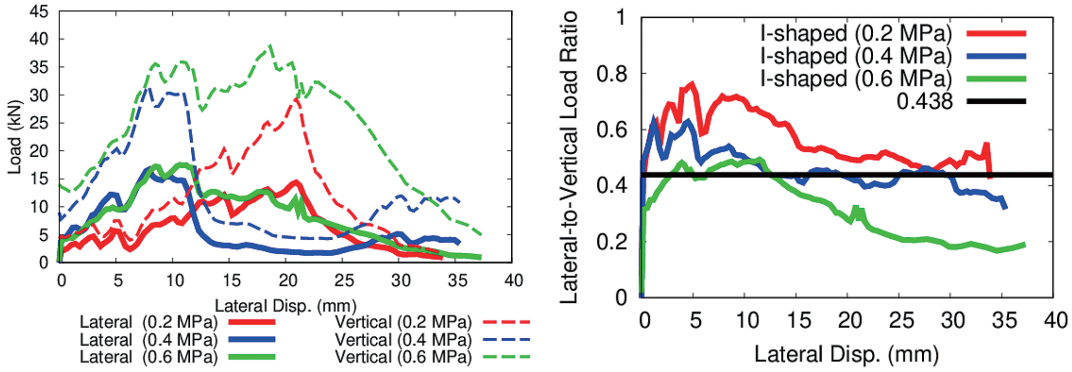

(a) (b)

Fig. 5 Test results for the I-shaped block wall: (a) load-displacement relationship; (b) relationship between the lateral-to-vertical load ratio and lateral displacement.

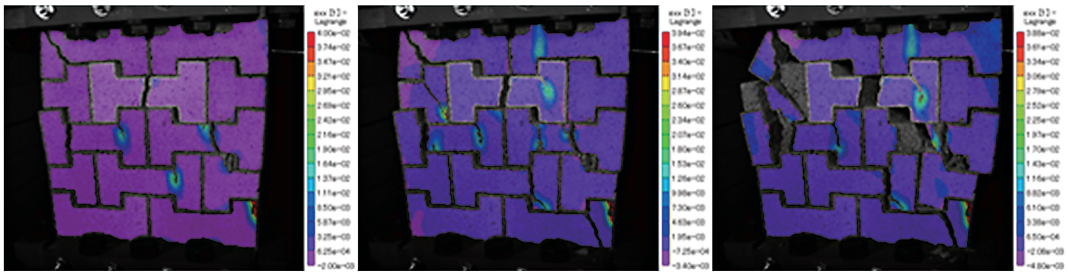

(a) (b) (c)

Fig. 6 Failure process and strain contour in the lateral direction of the I-shaped block wall with an initial vertical stress of 0.2 N/mm^2: (a) lateral displacement of 10 mm; (b) lateral displacement of 21 mm; (c) lateral displacement of 34 mm.

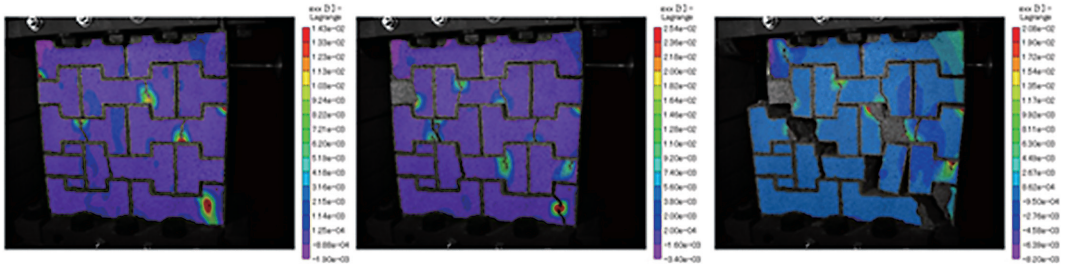

(a) (b) (c)

Fig. 7 Failure process and strain contour in the lateral direction of the I-shaped block wall with an initial vertical stress of 0.4 N/mm^2: (a) lateral displacement of 8 mm; (b) lateral displacement of 12 mm; (c) lateral displacement of 30 mm.

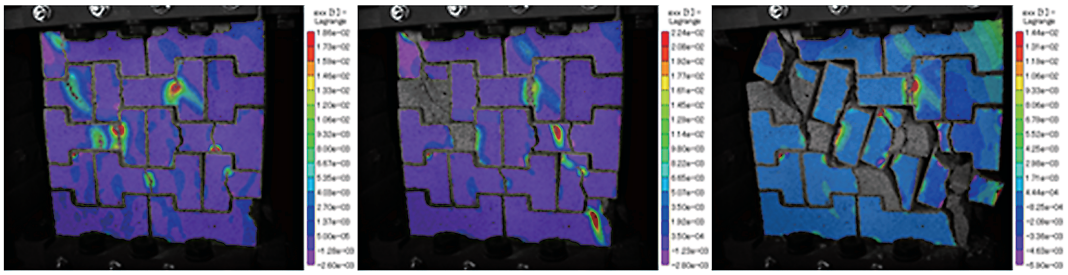

(a) (b) (c)

Fig. 8 Failure process and strain contour in the lateral direction of the I-shaped block wall with an initial vertical stress of 0.6 N/mm^2: (a) lateral displacement of 8 mm; (b) lateral displacement of 12 mm; (c) lateral displacement of 36 mm.

lateral-to-vertical load ratio when the strain inside the brick was smaller than the yield strain. However, cracks appeared at the interlocking parts when the strain exceeded the yield strain as the lateral displacement increased. Finally, after the maximum strength was reached, the interlocking mechanism stopped and sliding behavior was observed as shown in **Fig. 6(c)**. We thought that the lateral-to-vertical load ratio reached 0.438 because only the friction force resisted the lateral load after the peak load. Moreover, we observed that the I-shaped interlocking blocks had the advantage of higher lateral strength at the initial vertical stress of 0.2 N/mm^2. However, this was accompanied by brick failure and brittle behavior was observed.

Next, the results for the initial vertical stress of 0.4 N/mm^2 were investigated. As shown in **Fig. 5(a, b)**, a maximum lateral strength of 18.3 kN was obtained at a lateral displacement of 8 mm. At the initial vertical stress of 0.4 N/mm^2, the maximum lateral strength was observed at a smaller lateral displacement, in comparison with the case wherein the initial vertical stress was 0.2 N/mm^2. At a displacement of approximately 12 mm, the lateral load suddenly decreased. Before 12 mm, the interlocking mechanism worked as shown in **Fig. 7(a, b)**, wherein strain concentration can be observed at the interlocking parts. After 12 mm, the interlocking mechanism stopped, owing to the failure of the interlocking blocks. Additionally, the sliding movement of the wall began as shown in **Fig. 7(c)**. As can be seen in **Fig. 5(b)**, the lateral-to-vertical load ratio was larger than the friction coefficient of 0.438 before 12 mm. However, it was approximately the same as the friction coefficient after 12 mm. Based on these observations, we determined that the interlocking block walls underwent a strengthening effect before the maximum lateral load. However, the interlocking mechanism stopped when the block's interlocking part broke, and the value of the lateral-to-vertical load ratio approached the value of the friction coefficient.

Finally, the results for the initial vertical stress of 0.6 N/mm^2 were investigated. As shown in **Fig. 5(a, b)**, a maximum lateral strength of 18.7 kN was obtained at a lateral displacement of 8 mm. As shown in **Fig. 7(a, b)**, the interlocking mechanism worked and increased the lateral resistance before 12 mm. However, after 12 mm, the interlocking mechanism stopped, owing to brick failure. Subsequently, collapsing behavior, rather than sliding behavior, was observed as shown in **Fig. 7(c)**. In **Fig. 5(c)**, the lateral-to-vertical load ratio for 0.6 N/mm^2 was lower than the friction coefficient of 0.438 after 12 mm.

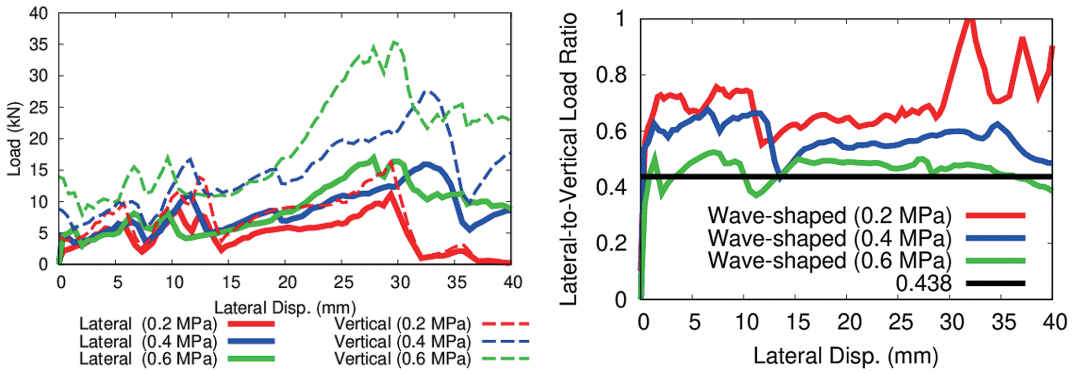

(a) (b)

Fig. 9 Test results for the wave-shaped block wall: (a) load-displacement relationship; (b) relationship between the lateral-to-vertical load ratio and lateral displacement.

(2) Discussion

The failure process of the I-shaped block wall without plaster can be divided into two stages. Before the maximum lateral load, the interlocking mechanism was in effect and the blocks resisted the lateral load by interlocking with each other. Additionally, the lateral strength increased in comparison with the rectangular block wall. The interlocking block suffered strain concentration at the interlocking parts, and block failure occurred at the interlocking parts when the strain exceeded the yield strain. After the maximum lateral load was reached, the interlocking part broke, the interlocking mechanism stopped working, and sliding movement or collapsing behavior was observed, depending on the vertical stress. The wall with a larger initial vertical stress had higher lateral strength, but exhibited more brittle behavior.

By comparing the lateral-to-vertical load ratios of the rectangular block wall with those of the I-shaped block wall, it was found that the I-shaped block wall had a higher lateral-to-vertical load ratio for a smaller initial vertical stress, and a lower lateral-to-vertical load ratio for a larger initial vertical stress. The effectiveness of using an I-shaped block wall was found to be dependent on the vertical stress.

3. 3 Wave-shaped block wall

(1) Results

First, we present the load-displacement relationship in **Fig. 9(a)**. Before the maximum lateral load was reached, several smaller peak loads were observed. At each peak load, cracks formed and caused the sudden decrease in the lateral load. After the maximum lateral strength was reached, the wall lost the interlocking mechanism, total failure occurred, and the lateral load suddenly decreased.

The lateral-to-vertical load ratio is presented in **Fig. 9(b)**. When the initial vertical stress was 0.2 N/mm^2, the lateral-to-vertical load ratio for the wave-shaped block wall was higher than that of the friction coefficient with a value of 0.438. This suggests that the interlocking mechanism increased the lateral strength. However, as the initial vertical stress increased, the effect of increasing the lateral-to-vertical load ratio decreased. The lateral-to-vertical load ratio was approximately 0.438 when the initial vertical stress was 0.6 N/mm^2.

Finally, the failure process and strain contour in the horizontal direction for the three cases are shown in **Figs. 10**, **11**, and **12**. Even though the

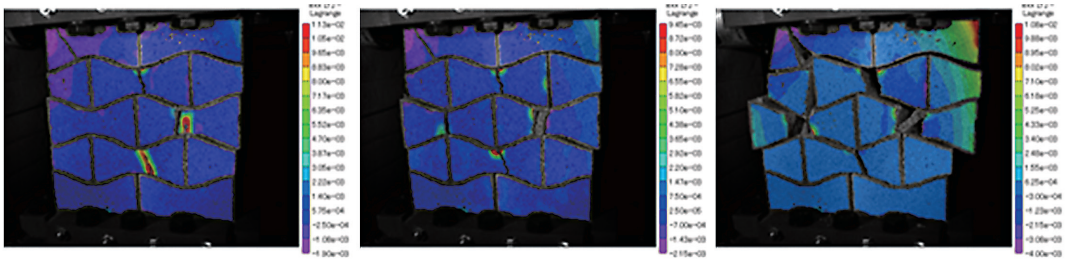

(a) (b) (c)

Fig. 10 Failure process and strain contour in the lateral direction of the wave-shaped block wall with an initial vertical stress of 0.2 N/mm^2: (a) lateral displacement of 30 mm; (b) lateral displacement of 35 mm; (c) lateral displacement of 40 mm.

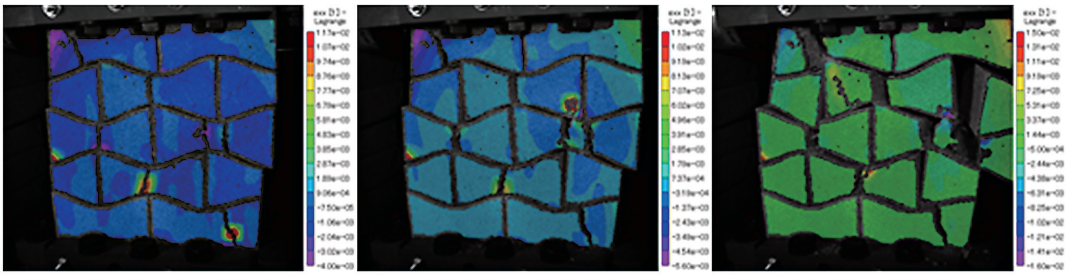

(a) (b) (c)

Fig. 11 Failure process and strain contour in the lateral direction of the wave-shaped block wall with an initial vertical stress of 0.4 N/mm^2: (a) lateral displacement of 18 mm; (b) lateral displacement of 33 mm; (c) lateral displacement of 36 mm.

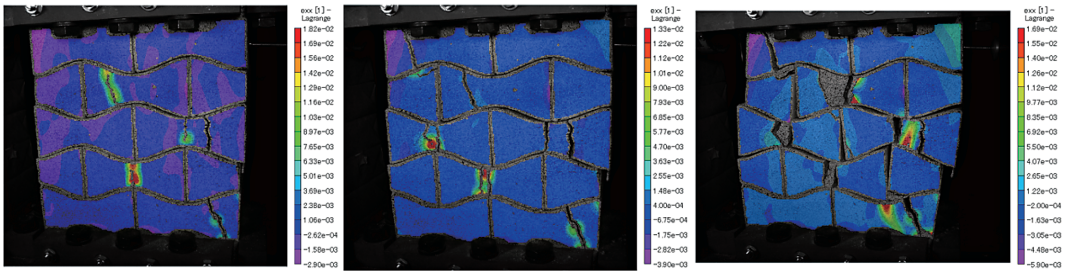

(a) (b) (c)

Fig. 12 Failure process and strain contour in the lateral direction of the wave-shaped block wall with an initial vertical stress of 0.6 N/mm^2: (a) lateral displacement of 27 mm; (b) lateral displacement of 30 mm; (c) lateral displacement of 40 mm.

cracked area and crack order are different for the three cases with different initial vertical stress, the constricted portions of the blocks were cracked. **Figs. 10(a)**, **11(a)**, and **12(a)** depict the failure situation at the peak load before the maximum lateral strength, where a large strain at the constricted portion of the blocks can be observed. Because of the interlocking between the elements, strain concentration occurred at the constricted portions. When a crack occurred at these constricted portions, the lateral load exhibited sudden drops. Then, the lateral load increased again, while the interlocking mechanism remained active. **Figs. 10(b)**, **11(b)**, and **12(b)** depict the failure situation at the maximum lateral strength, when the last constricted portion cracked and the interlocking mechanism was lost. After the wall lost the interlocking mechanism, the lateral load decreased drastically and the movement of the wall proceeded as shown in **Figs. 10(c)**, **11(c)**, and **12(c)**.

(2) Discussion

The failure process of the wave-shaped block wall without plaster can be divided into two stages, in the same manner as the I-shaped block wall. Before the maximum lateral load, the interlocking mechanism was in effect and the blocks resisted the lateral load by interlocking with each other. Additionally, the lateral strength increased in comparison with the rectangular block wall. The interlocking block suffered strain concentration at the constricted parts, and block failure occurred at the constricted parts. The lateral load decreased when block failure occurred; however, the lateral load increased and the interlocking mechanism remained active. After the interlocking mechanism was lost, the increase in lateral displacement became easier. The wall with a larger initial vertical stress had a higher lateral strength, but lower lateral-to-vertical load ratios. The effectiveness of using a wave-shaped block wall was found to be dependent on the vertical stress.

3. 4 Comparison of block shape effect

Fig. 13 shows the effect of the block shape on the load-displacement relationship and the lateral-to-vertical load ratio. **Table 3** presents a comparison of the maximum lateral strength with lateral displacement, where the maximum lateral strength was observed. The lateral displacement is not shown for the rectangular block wall.

Moreover, it was found that the rectangular block wall exhibited sliding movement under the resistance of friction force. Additionally, the lateral load and the lateral-to-vertical load ratio were approximately constant throughout the lateral loading. However, the I-shaped block wall and the wave-shaped block wall had several peaks in their load-displacement relationships. These peaks corresponded to the failure of the block at the interlocking parts. In comparison with the I-shaped block wall, the wave-shaped block wall had a slightly smaller maximum load; however, that maximum load was observed at a larger displacement. The wave-shaped block wall had a larger lateral load at a larger lateral displacement, in comparison with the I-shaped block wall.

When we compared the lateral-to-vertical load ratios, we found that the rectangular block wall had the lowest such ratio at the initial vertical strength of 0.2 N/mm^2. However, the same value was generally the lowest for the I-shaped block wall at the initial vertical strength of 0.6 N/mm^2. The lateral-to-vertical load ratio of the rectangular block wall was approximately constant, regardless of the initial vertical stress, because the resisting force was the friction force. Conversely, the lateral-to-vertical load ratio of the I-shaped block wall decreased as the initial vertical stress increased, because the strain concentration at the interlocking parts was increased by the vertical stress. An I-shaped block wall can easily suffer from strain

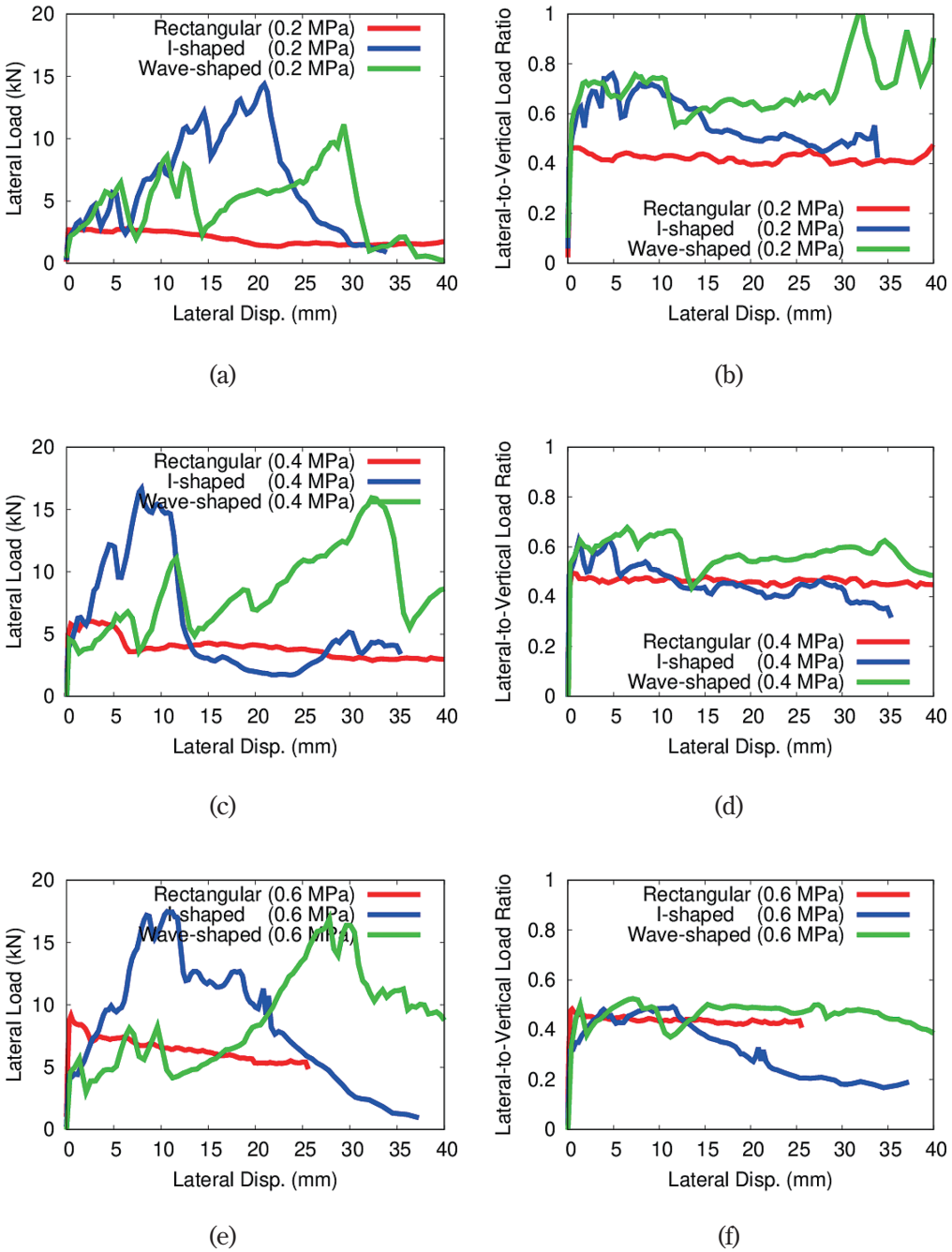

Fig. 13 Test results for different block shapes with the same initial vertical stress: (a) load-displacement relationship (0.2 N/mm^2); (b) relationship between the lateral-to-vertical load ratio and lateral displacement (0.2 N/mm^2); (c) load-displacement relationship (0.4 N/mm^2); (d) relationship between the lateral-to-vertical load ratio and lateral displacement (0.4 N/mm^2); (e) load-displacement relationship (0.6 N/mm^2); (f) relationship between the lateral-to-vertical load ratio and lateral displacement (0.6 N/mm^2).

Table 3 Maximum lateral strength (lateral displacement where maximum lateral strength occurred for the I-shaped and wave-shaped block walls).

Initial vertical stress	Rectangular block wall	I-shaped block wall	Wave-shaped block wall
0.2 N/mm^2	2 kN	15.3 kN (21 mm)	12.4 kN (29 mm)
0.4 N/mm^2	4 kN	18.3 kN (8 mm)	17.3 kN (32 mm)
0.6 N/mm^2	7 kN	18.7 kN (8 mm)	18.4 kN (28 mm)

concentration, and cracks may occur under larger vertical stress. The wave-shaped block wall had the highest lateral-to-vertical load ratio amongst the three block shapes, regardless of the initial vertical stress. Similar to the I-shaped block wall, the wave-shaped block wall also suffered from strain concentration at the constricted portions. However, the strain concentration was smaller, owing to this wall's smooth shape at the interface.

Let us compare the strain contour in the lateral direction at the maximum lateral load for the I-shaped block wall (**Figs. 8(b)**, **9(b)**, and **10(b)**) and the wave-shaped block wall (**Figs. 12(b)**, **13(b)**, and **14(b)**), when the initial vertical stresses were 0.2 N/mm^2, 0.4 N/mm^2, and 0.6 N/mm^2, respectively. Although it is difficult to read the values from the figures, the maximum values (tensile strain) for the I-shaped block wall were 3.94×10^{-2}, 2.54×10^{-2}, and 2.24×10^{-2}, while those for the wave-shaped block wall were 9.45×10^{-3}, 1.13×10^{-2}, and 1.33×10^{-2}. Based on this tensile strain comparison, the wave-shaped block was effective in reducing the strain concentration, owing to its smooth shape at the interface.

From the comparison, it was determined that the interlocking block walls were effective relative to the rectangular block walls for a small initial vertical stress, because the friction force was small. However, as the initial vertical stress increased, the effectiveness of the interlocking blocks decreased, particularly for the I-shaped block wall. The wave-shaped block wall had an advantage in comparison with the I-shaped block wall, because the wave-shaped block wall had larger lateral resistance and a higher lateral-to-vertical load ratio at a larger lateral displacement, owing to its smooth shape. This study could reveal the effectiveness of using interlocking blocks under different vertical stress conditions owing to the in-plane loading tests, which was impossible in previous studies using diagonal compression tests.

4. Conclusions

In this study, a lateral loading test was conducted for mortarless masonry walls, namely a rectangular block wall, I-shaped block wall, and wave-shaped block wall, under three levels of initial vertical stress.

The rectangular block wall exhibited sliding movement at the location where the friction force resisted the lateral loading. Therefore, the lateral load and lateral-to-vertical load ratio were approximately constant throughout the loading without cracks appearing, regardless of the initial vertical stress. The rectangular wall with a larger initial vertical stress had a higher lateral strength. Conversely, the load-displacement relationships for the I-shaped block wall and the wave-shaped block wall had several peaks. Because of the interlocking mechanism, strain concentration occurred at the interlocking part, where cracking occurs more easily in comparison with other parts. Moreover, when a block cracks, the lateral load decreases.

The lateral load increased again while the interlocking mechanism was in effect. Total failure occurred after the interlocking mechanism was lost. Under a small initial vertical load, which implies a small friction force, the I-shaped block and wave-shaped block walls exhibited a higher lateral-to-vertical load ratio in comparison with

the rectangular block wall. However, as the initial vertical stress increased, the increasing effect of the lateral-to-vertical load ratio decreased, particularly for the I-shaped block wall. The wave-shaped block wall had the maximum lateral strength at the longer lateral displacement, in comparison with the I-shaped block wall, because the strain concentration was smaller as a result of the smooth shape at the interface. The comparison results revealed that the wave-shaped block wall had better performance in terms of higher strength and larger displacement. Additionally, the interlocking block walls were not effective under a larger initial vertical stress.

In future work, we will consider the effect of plaster between the blocks, and investigate the effective shape of interlocking blocks with higher strength and better ductility. It is possible that the advantage of the wave-shaped block wall with lower stress concentration is reduced if there is plaster between blocks. Therefore, we would like to investigate the most advantageous block shape with the existence of plaster.

Moreover, this study only focused on the in-plane collapse behavior of the masonry walls. We would like to investigate the effectiveness of interlocking block walls regarding the out-of-plane collapse behavior and three-dimensional collapse behavior in our future study.

Acknowledgements

We would like to thank Professor Shiotani, Professor Nishida, Professor Asaue, and Professor Hashimoto from Kyoto University for letting us use the digital correlation systems and for providing valuable assistance during the experiment. This study was supported in part by the Japan Society for the Promotion of Science (JSPS) grant-in-aid (15K06178,18K04323), whose support is greatly appreciated.

References

Coburn, A., Spence, R. Earthquake protection, 2nd edition. Chichester: John Wiley and Sons, 2002.

Corelated Solutions. The VIC3D System. http://correlatedsolutions.com/vic-3d/. [Accessed June 20, 2018]

Darbhanzi, A., Marefat, M. S., Khanmohammadi, M. Investigation of in-plane seismic retrofit of unreinforced masonry walls by means of vertical steel ties. Construction and Building Materials, Vol. 52, pp. 122–129, 2014.

Furukawa, A., Kimura, S., Kiyono, J. Study on failure mechanism and strength increment effect of masonry walls made of interlocking bricks. Journal of Japan Society of Civil Engineers, Ser. A1 (Structural Engineering & Earthquake Engineering (SE/EE)), Vol. 74, Issue 4, pp. I_699-I_711, 2018a. https://doi.org/10.2208/jscejseee.74.I_699.

Furukawa, A., Masuda, K., Daru, G.T.S., Kiyono, J. Shape effect of interlocking blocks on force-displacement relationship and failure behavior of masonry wall. Journal of Structural Engineering, Vol. 64A, pp. 241–249, 2018b.

Giardini, D., Gruenthai, G., Shedlock, K., Zhang, P. The GSHAP global seismic hazard map, in: W. HK. Lee, H. Kanamori, P.C. Jennings, C. Kisslinger (Eds.). International Handbook of Earthquake and Engineering Seismology, Vol. 81B, London, U.K.: Academic Press, pp. 1233–1239, 2003.

Marcari, G., Manfredi, G., Prota, A., Pecce, M. In-plane shear performance of masonry panels strengthened with FRP. Composites: Part B, Vol. 38, pp. 887–901, 2007.

Navaratnarajah S., Kotaro S., Kimiro M. Experimental study of PP-band retrofitted masonry structure made of shapeless stone. SEISAN-KENKYU, Vol. 61, Issue 6, pp. 1051–1054, 2009.

OCHA (Office for the Coordination of Humanitarian Affairs). http://www.unocha.org/, 2015. [Accessed June 20, 2018]

Sanada, Y., Nakamura, Y., Yamauchi, N., Akano, Y. Seismic performance of masonry walls using interlocking units. Proceedings of the First European Conference on Earthquake Engineering and Seismology, Paper No. 508, 2006.

Turer, A., Golalm, M. Scrap tire as low-cost post

tensioning material for masonry strengthening. Materials and Structures, Vol. 41, pp. 1345–1361, 2011.

Yamaguchi, K., Amiraslanzadeh, R., Ikemoto, T., Fukada, S., Miyajima, M., Murata, A. The static loading test on earthquake effect of reinforcing the block wall model. Journal of Disaster Mitigation for Historical Cities, Vol. 8, pp. 243–248, 2014.

（投 稿 受 理：2019年 3 月 1 日
訂正稿受理：2019年 7 月 3 日）

要　旨

組積造壁の面内水平載荷試験により，インターロッキングブロックを用いた組積造の補強効果について検証を行った。一般的な直方体のブロックと，I 型の形状をしたインターロッキングブロック，波型の形状をしたインターロッキングブロックの 3 種類のブロックから構成される 3 種類の組積造壁を試験対象とした。2 階建，4 階建，6 階建の組積造建物の 1 階の壁が支える上載荷重を想定し，3 通りの鉛直応力に対して試験を行った。試験の結果，上載荷重が小さい場合にインターロッキング組積造壁は直方ブロック組積造壁よりも強度が高いことが明らかとなった。上載荷重が増えるにつれて，摩擦力が増加し，直方ブロック組積造壁の強度が相対的に上昇するため，インターロッキング組積造壁の効果が減少することがわかった。